Supporting Information

Freestanding Carbon-nanotubes-modified Graphitic Carbon Foam Film as a Flexible Anode for Potassium Ion Batteries

*Sifan Zeng[1, 2, 3], Xuefeng Zhou[2], Bin Wang[2], Yuezhan Feng,[5] Rui Xu[2], Haibin Zhang[1, *], Shuming Peng[1, 3, *], Yan Yu[2, 4*]*

[1] Innovation Research Team for Advanced Ceramics, Institute of Nuclear Physics and Chemistry, China Academy of Engineering Physics, Mianyang, 621900, Sichuan, China. E-mail: hbzhang@caep.cn, pengshuming@caep.cn

[2] Hefei National Laboratory for Physical Sciences at the Microscale, Department of Materials Science and Engineering, Key Laboratory of Materials for Energy Conversion, Chinese Academy of Sciences (CAS), University of Science and Technology of China, Hefei, Anhui, 230026, China. Email: yanyumse@ustc.edu.cn

[3] Department of Engineering and Applied Physics, University of Science and Technology of China, Hefei, 230026, China

[4] Dalian National Laboratory for Clean Energy (DNL), Chinese Academy of Sciences (CAS), Dalian 116023, China

[5] Key Laboratory of Materials Processing and Mold, Ministry of Education, Zhengzhou University, Zhengzhou 450002, China

Experimental Section

Synthesis of GCF. The GCF was prepared by a chemical vapor deposition method with commercial nickel foam as a template. A mixed gas of CH_4, H_2, and Ar at flowing rates of 50, 50 and 200 sccm passed through Ni foam at 1000 ^oC holding 5 min in the tube furnace. And then, the sample was etched by $FeCl_3$/HCl mixed solution after cooled down naturally. Lastly, the GCF was obtained after washing three times by deionized water and drying at 60 ^oC for 12 h.

Synthesis of CNTs-modified GCF. Firstly, the GCF film was immersed into 60 mL of mixed solution with 0.15 mmol $Ni(NO_3)_2 \cdot 6H_2O$, 0.3 mmol $Co(NO_3)_2 \cdot 6H_2O$ and 1.8 mmol urea. After holding 120 ^oC for 2 h in an autoclave, NiCo@GCF precursor was annealed in air at 350 ^oC for 1 min and subsequently used as a catalyst-loaded substrate for growth of CNTs at 750 ^oC for 10 min in C_2H_4, H_2 and Ar atmosphere with the rates of 50, 50 and 200 sccm. Finally, the CNTs/GCF film was collected after etching in HCl solution, washing by deionized water and drying at 60 ^oC for 12 h.

Materials characterization. The electrical conductivity of the composites was measured by a four-probe method. The morphologies of the materials were investigated by Field-emission scanning electron microscopy (FESEM,). Transmission Electron Microscope (JEM-2100F, JEOL, Japan) was employed to measure TEM and HRTEM. The compositions of samples were studied by the X-Ray diffraction (XRD) by a Rigaku D/max-RB12 X-Ray diffractometer with Cu Kα radiation. The Raman spectra were tested through a microscopic confocal Raman spectrometer (Renishaw RM2000) with a wavelength of 514 nm at room temperature. In-situ Raman spectra were measured by a Raman spectrometer (Horiba) with a wavelength of 633nm.

Electrochemical measurements. 2032-type coin cells were assembled in an argon-filled glove box. The free-standing CNTs/GCF and GCF films were used as working electrodes coupled with K metal. Glass fiber (Whatman) was used as separators. The electrolyte solutions used in this work was 0.7M KPF6 in a 1:1 (v/v) mixture of ethylene carbonate (EC) and diethyl carbonate (DEC). The galvanostatic charge-discharge tests were performed at different current densities within a voltage interval of 0.01-2.5 V. Cyclic voltammograms (CVs) scanned in a voltage window of 0.01-2.5 V at 0.2 mV/s and electrochemical impedance spectrum (EIS) in the frequency range of 100 kHz to 0.01 Hz was measured by an electrochemical station (CHI618D).

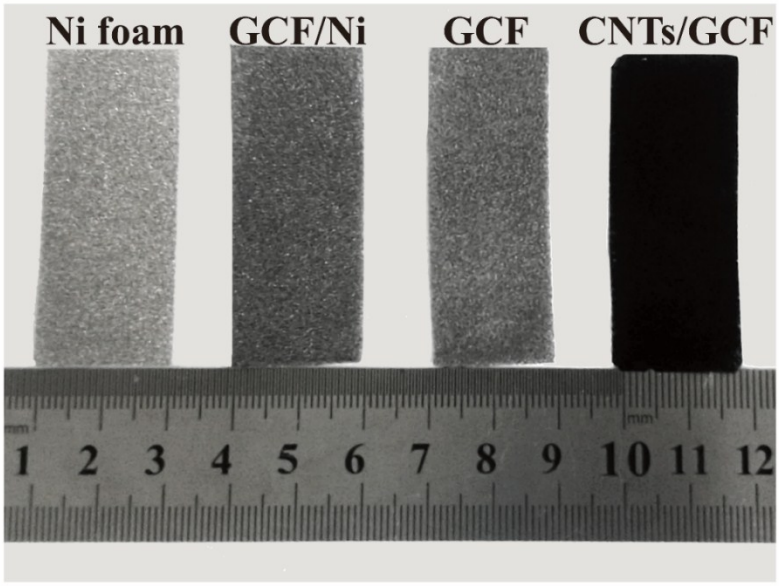

Figure S1. Optical images of inch-scaled Ni foam, GCF/Ni, GCF and CNTs/GCF.

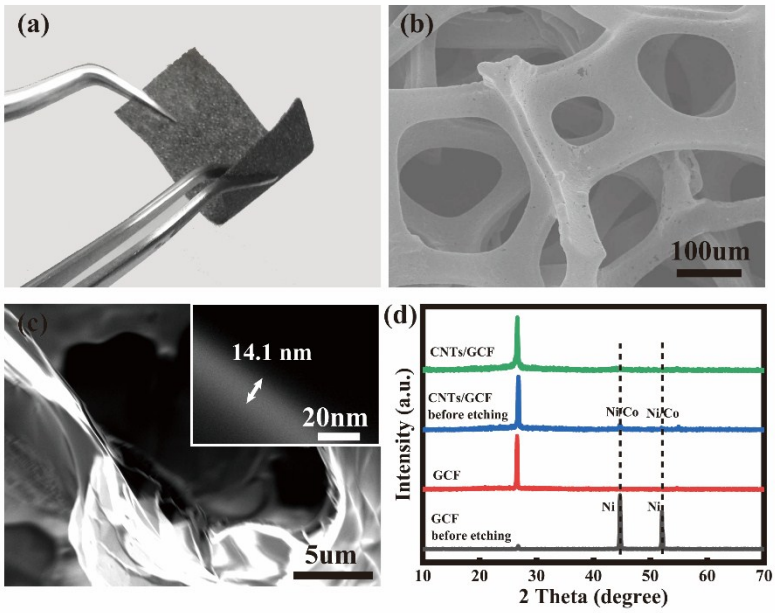

Figure S2. The SEM images of GCF film, (a) Optical, (b) top view, (c) cross-section view, (inset of (c)) single layer. (d) XRD patterns of all specimens before and after HCl etching

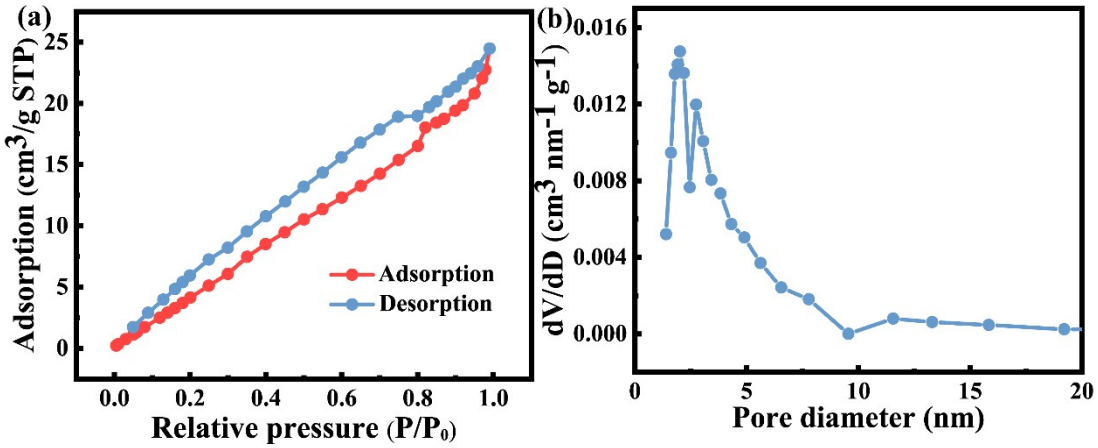

Figure S3. (a) N_2 adsorption-desorption curves and (b) pore size distribution of GCF

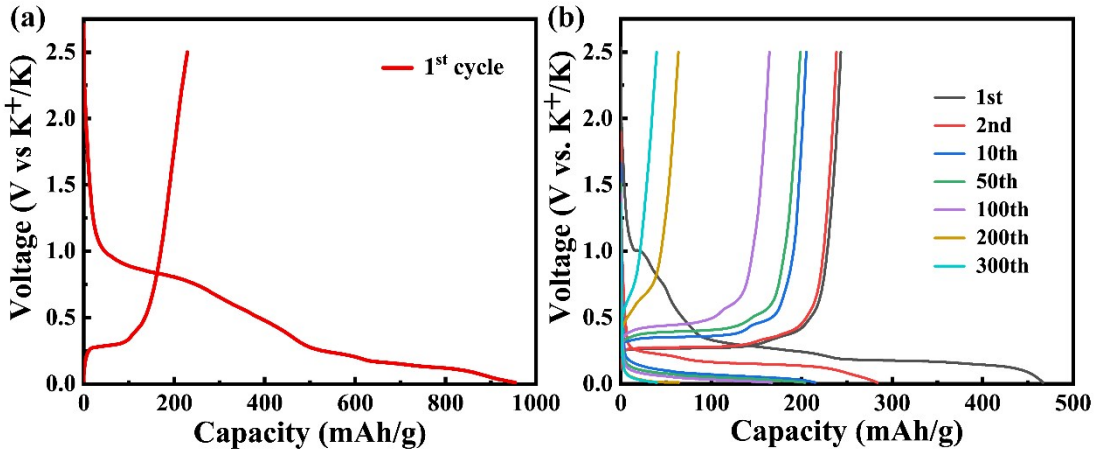

Figure S4. (a) The first discharge and charge profiles of CNTs/GCF and (b) Voltage profiles of GCF at 100 mA/g.

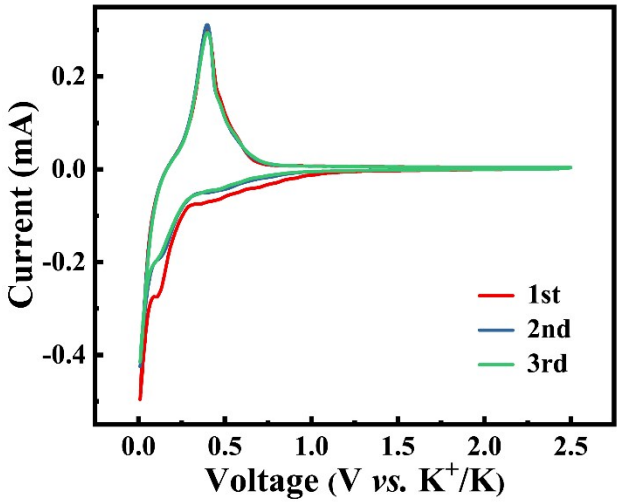

Figure S5. The CV curves of GCF at the scan rate of 0.2 mV/s.

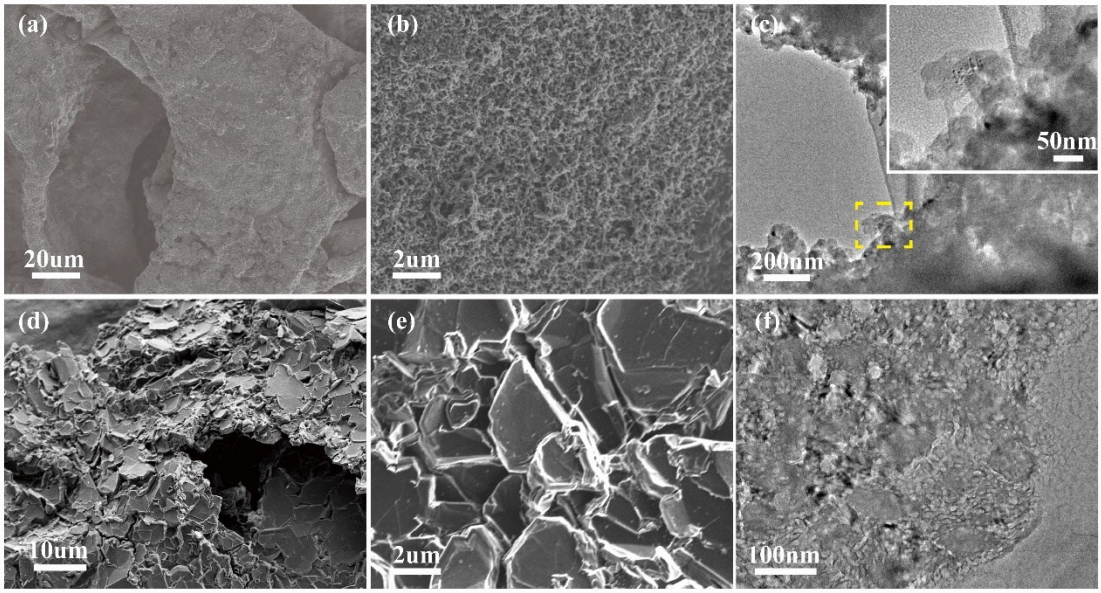

Figure S6. The morphology of CNTs/GCF and GCF films after cycles. (a, b) SEM and (c) TEM images of CNTs/GCF, (d, e) SEM and (f) TEM images of GCF.

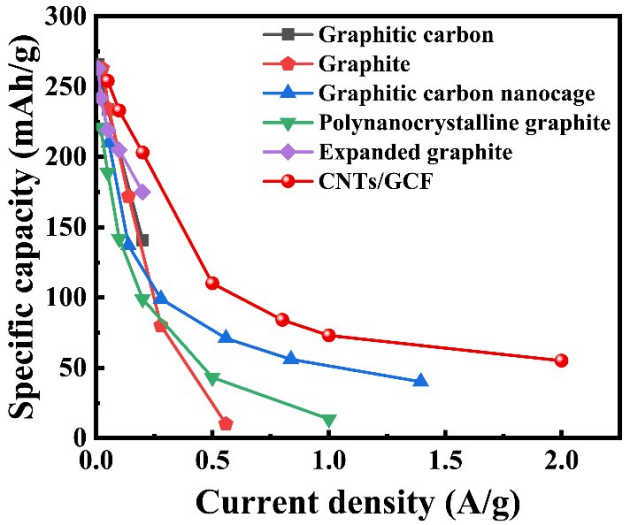

Figure S7. Comparison of rate capability with the reported graphitic carbon materials for KIBs.

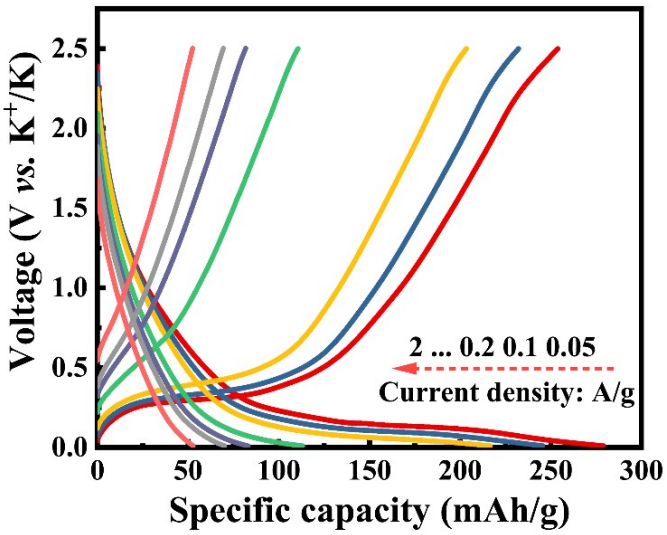

Figure S8. The discharge/charge profiles of CNTs/GCF at different current densities.

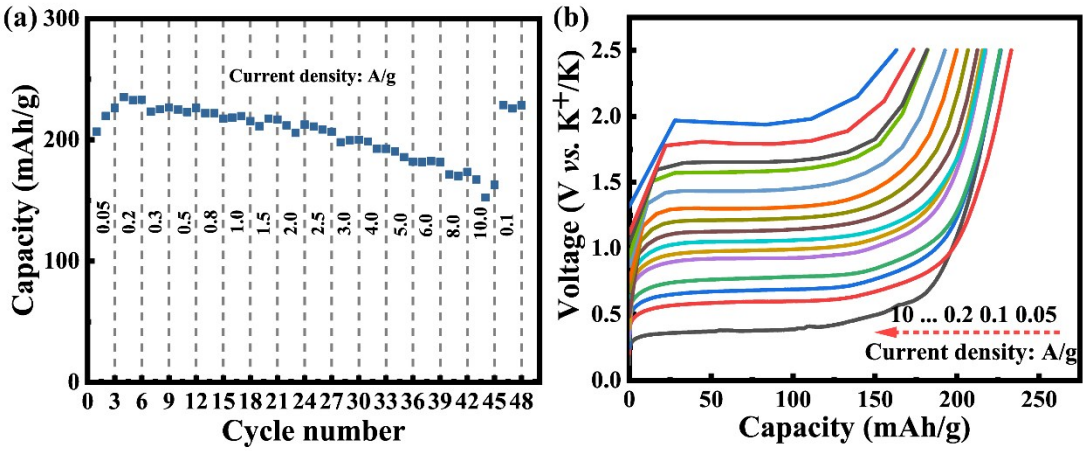

Figure S9. (a) The depotassiation capability with rate capability and (b) voltage profiles at different rates of GCF.

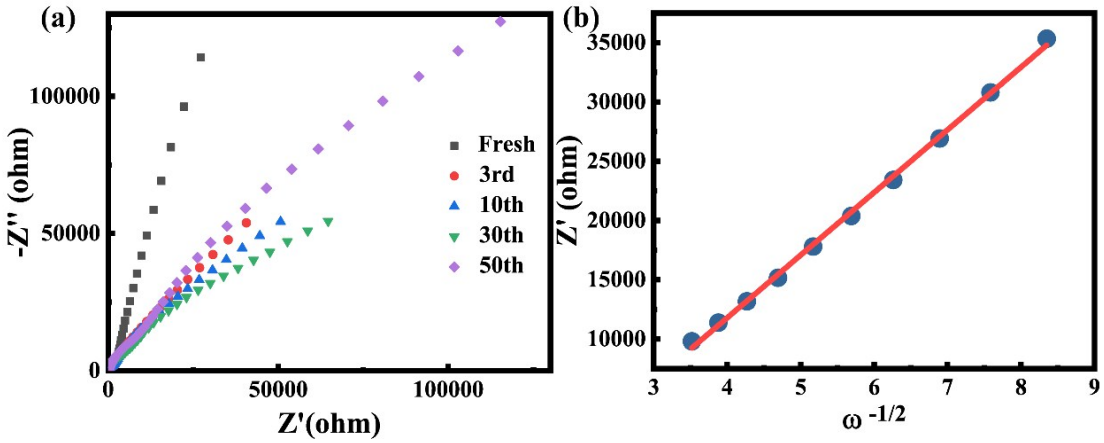

Figure S10. (a) EIS curves and (b) linear fits of Z′ versus $\omega^{-1/2}$ of GCF.

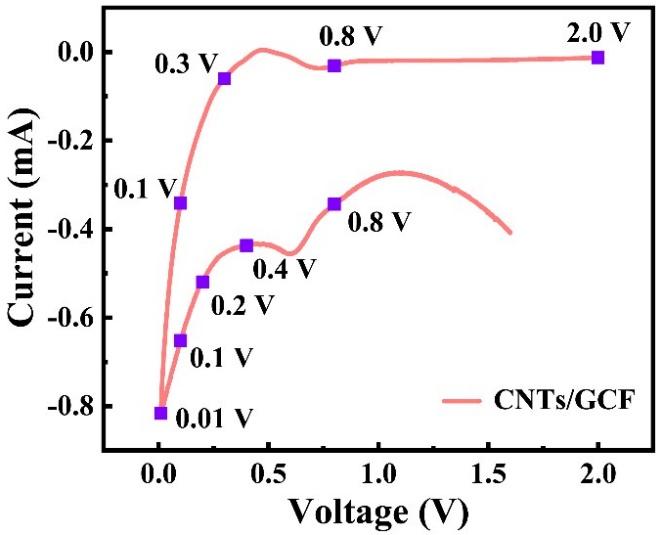

Figure S11. The first CV cycle of CNTs/GCF obtained from *in-situ* Raman experiments.

Table S1. Comparison of Carbon-based KIBs anodes reported in the literature

Materials	Current Density (mA/g)	Cycle Number	After Cycles Capacity below 0.25 V (mAh/g)	After Cycles Capacity (mAh/g)	Reference
Graphite	6.975	2	~255	325	[1]
N-doped CNTs mats	20	5	~195	350	[2]
N-doped bamboo-like CNTs	500	10	~270	420	[3]
S-doped rGO	50	50	~70	361	[4]
Graphitic carbon nanocage	55.8	50	~125	210	[5]
N-doped carbon fibers	55.8	100	~65	215	[6]
S, O-doped hard carbon	50	100	~76	226	[7]
Short-ordered mesoporous carbon	50	100	~57	257	[8]
N, O-doped hard carbon	50	100	~60	230.6	[9]
Expanded graphite	50	200	~200	228	[10]
Hard-soft carbon	55.8	440	~100	200	[11]
N-doped porous carbon	100	500	~82	342	[12]
Hierarchical CNTs	100	500	~70	210	[13]
Activated hollow carbon nanospheres	2000	1000	~45	190	[14]
CNTs/GCF	100	2	258	332.9	This work
	100	500	138	205	
	100	800	143.5	228	

Reference

1. Z. Jian, W. Luo, X. Ji, *J. Am. Chem. Soc.* **2015**, 137, 11566.
2. X. Zhao, Y. Tang, C. Ni, J. Wang, A. Star, Y. Xu, *ACS Appl. Mater. Interfaces* **2018**, 1, 1703.
3. Y. Liu, C. Yang, Q. Pan, Y. Li, G. Wang, X. Ou, F. Zheng, X. Xiong, M. Liu, Q. Zhang, *J. Mater. Chem. A* **2018**, 6, 15162.
4. J. Li, W. Qin, J. Xie, H. Lei, Y. Zhu, W. Huang, X. Xu, Z. Zhao, W. Mai, *Nano Energy* **2018**, 53, 415.
5. B. Cao, Q. Zhang, H. Liu, B. Xu, S. Zhang, T. Zhou, J. Mao, W. K. Pang, Z. Guo, A. Li, *Adv.d Energy Mater.* **2018**, 8, 1801149.
6. R. Hao, H. Lan, C. Kuang, H. Wang, L. Guo, *Carbon* **2018**, 128, 224.
7. M. Chen, W. Wang, X. Liang, S. Gong, J. Liu, Q. Wang, S. Guo, H. Yang, *Adv. Energy Mater.* **2018**, 1800171.
8. W. Wang, J. Zhou, Z. Wang, L. Zhao, P. Li, Y. Yang, C. Yang, H. Huang, S. Guo, *Adv. Energy Mater.* **2018**, 8, 1701648.
9. J. Yang, Z. Ju, Y. Jiang, Z. Xing, B. Xi, J. Feng, S. Xiong, *Adv. Mater.* **2018**, 30, 1700104.
10. Y. An, H. Fei, G. Zeng, L. Ci, B. Xi, S. Xiong, J. Feng, *J. Power Sources* **2018**, 378, 66.
11. Z. Jian, S. Hwang, Z. Li, A. S. Hernandez, X. Wang, Z. Xing, D. Su, X. Ji, *Adv. Funct. Mater.* **2017**, 27, 1700324.
12. D. Li, X. Ren, Q. Ai, Q. Sun, L. Zhu, Y. Liu, Z. Liang, R. Peng, P. Si, J. Lou, *Adv. Energy Mater.* **2018**, 1802386.
13. Y. Wang, Z. Wang, Y. Chen, H. Zhang, M. Yousaf, H. Wu, M. Zou, A. Cao, R. P. Han, *Adv. Mater.* **2018**, 30, 1802074.
14. G. Wang, X. Xiong, D. Xie, Z. Lin, J. Zheng, F. Zheng, Y. Li, Y. Liu, C. Yang, M. Liu, *J. Mater. Chem. A* **2018**.